Int. J. Morphol.,
39(3):732-738, 2021.

Liver Structural Injury in Leptin-Deficient (*ob*/*ob*) Mice: Lipogenesis, Fibrogenesis, Inflammation, and Apoptosis

Lesión Estructural del Hígado en Ratones con Deficiencia de Leptina (*ob*/*ob*): Lipogénesis, Fibrogénesis, Inflamación y Apoptosis

Fabiane Ferreira Martins[1]; Vanessa Souza-Mello[1]; Jorge Jose de Carvalho[2]; Mariano del Sol[3]; Marcia Barbosa Aguila[1] & Carlos Alberto Mandarim-de-Lacerda[1]

MARTINS, F. F.; SOUZA-MELLO, V.; CARVALHO, J. J.; DEL SOL, M.; AGUILA, B. M. & MANDARIM-DE-LACERDA, C. A. Liver structural injury in leptin-deficient *(ob/ob)* mice: Lipogenesis, fibrogenesis, inflammation and apoptosis. *Int. J. Morphol., 39(3)*:732-738, 2021.

SUMMARY: Nonalcoholic fatty liver disease (NAFLD) might progress the steatosis to nonalcoholic steatohepatitis (NASH), reaching a cirrhosis state and possibly hepatocellular carcinoma. The liver of three-month-old C57BL/6J mice (wild-type, WT group, n=10) and leptin-deficient obese mice (*ob*/*ob* group, n=10) were studied, focusing on the mechanisms associated with the activation of the hepatic stellate cells (HSCs) and pro-fibrogenesis. The obese *ob*/*ob* animals' liver showed steatosis, increased lipogenesis gene expressions, inflammation, increased pro-inflammatory gene expressions, inflammatory infiltrate, and potential apoptosis linked to a high Caspase 3 expression. In *ob*/*ob* mice, liver sections were labeled in the fibrotic zones by anti-alpha-smooth muscle actin (alpha-SMA) and anti-Reelin, but not in the WT mice. Moreover, the alpha-SMA gene expression was higher in the *ob*/*ob* group's liver than the WT group. The pro-fibrogenic gene expressions were parallel to anti- alpha-SMA and anti-Reelin immunofluorescence, suggesting HSCs activation. In the *ob*/*ob* animals, there were increased gene expressions involved with lipogenesis (Peroxisome proliferator-activated receptor-gamma, Cell death-inducing DFFA-like effector-c, Sterol regulatory element-binding protein-1c, and Fatty acid synthase), pro-fibrogenesis (Transforming growth factor beta1, Smad proteins-3, Yes-associated protein-1, Protein platelet-derived growth factor receptor beta), pro-inflammation (Tumor necrosis factor-alpha, and Interleukin-6), and apoptosis (Caspase 3). In conclusion, the results in obese *ob*/*ob* animals provide a clue to the events in humans. In a translational view, controlling these targets can help mitigate the hepatic effects of human obesity and NAFLD progression to NASH.

KEY WORDS: Steatosis; Stellate cell; Fibrosis; Confocal microscopy; Stereology.

Abbreviations

SMA, actin smooth muscle; Cide, cell death-inducing DFFA-like effector; Col1a1, type I collagen; ELISA, enzyme-linked immunosorbent assay; Fas, fatty acid synthase; HE, hematoxylin and eosin; HSCs, hepatic stellate cell; Il 6, interleukin 6; NAFLD, nonalcoholic fatty liver disease; NASH, nonalcoholic steatohepatitis; *ob*/*ob*, leptin-deficient obese mouse; Pdgfr, protein platelet-derived growth factor receptor; Ppar, peroxisome proliferator-activated receptor; RT-qPCR, real-time quantitative polymerase chain reaction; Smad, smad proteins; Srebp, sterol regulatory element-binding protein; Tgf, transforming growth factor; Tnf, tumor necrosis factor; WT, wild-type; Yap, Yes-associated protein.

INTRODUCTION

Leptin-deficient mouse (*ob*/*ob*) develops liver steatosis (comparable with the nonalcoholic fatty liver disease or NAFLD in humans). The pro-inflammatory state might progress the steatosis to nonalcoholic steatohepatitis (or NASH in humans), which, associated with fibrogenic processes in the long-term, may result in the deposition of excess matrix tissue and liver fibrosis (Bettermann *et al*., 2014).

The hepatic stellate cells (HSCs) are the dominant source of hepatic myofibroblasts (Lua *et al*., 2016). Improved fibrillar elements are produced by HSCs, modulated by pro-fibrotic factors, and accumulated in the extracellular matrix (ECM) in liver fibrosis (Sferra *et al*., 2017). The liver fibrosis pathogenesis starts with the HSCs activation to repair the damage, depositing collagen in the stroma, a process dependent on modulating cytokine induction and inflammation (Zhang *et al*., 2020). However, HSCs might remain activated depending on the stimuli, and liver fibrosis progresses, reaching a cirrhosis situation (Khomich *et al*., 2019) and possibly hepatocellular carcinoma (Martin *et al*., 2020).

[1]Laboratory of Morphometry, Metabolism, and Cardiovascular Diseases, Biomedical Center, Institute of Biology, The University of the State of Rio de Janeiro, Rio de Janeiro, Brazil.
[2]Laboratory of Ultrastructure and Tissue Biology. Biomedical Centre, Institute of Biology, The University of the State of Rio de Janeiro, Rio de Janeiro, Brazil.
[3]Doctoral Program in Morphological Sciences, Universidad de La Frontera, Temuco, Chile.

The liver adaptation to nutrient excess, obesity, and HSCs activation are complex processes that involve biochemical, molecular, and immunological mechanisms (Fuchs *et al*., 2020). Activated HSCs change into myofibroblast-like cells and express alpha-SMA in response to liver injury (Carpino *et al*., 2005), and participate in hepatic inflammation by releasing a set of inflammatory cytokines and chemokines (Gupta *et al*., 2019).

Because of its central involvement in liver fibrosis' pathogenesis and its link with pro-fibrogenic pathways, new therapies for NAFLD/NASH might be expected regarding the HSCs. The anti-fibrotic drugs (e.g., pirfenidone and nintedanib), active via transforming growth factor (TGF) beta, still have related mechanisms not entirely known (Cho, 2018).

The study aimed to understand better the pathways linked to lipogenesis, HSCs activation, pro-fibrogenesis, pro-inflammation, and apoptosis in *ob/ob* mouse, which might help understand hepatic progression steatosis to a stage of steatohepatitis, with translation to the disease in humans.

MATERIAL AND METHOD

Experimental protocol. The current animal experiment complies with the ARRIVE guidelines and NIH Publication number 85-23 (revised 1996). The local Ethics Committee approved procedures (Protocol number CEUA 010/2016).

One-month-old male *ob/ob* and C57BL/6J mice (as the control group, wild-type, WT) stemmed from a colony derived from the Jackson Laboratory (B6.V-Lepob/J, stock no. 000632, Bar Harbor, ME, USA). The animals were kept in ventilated cages under controlled conditions (Nexgen system, Allentown Inc., PA, USA, 21 ± 2 °C, and 12 h/12 h dark/light cycle), with free access to food and water until three months of age (n= 10/group), feeding a balanced diet (10 % KJ lipids, 14 % KJ proteins, 76 % KJ carbohydrates) (Aguila *et al*., 2021).

Sacrifice. Animals were anesthetized (sodium pentobarbital 150 mg/kg, intraperitoneal) and exsanguinated (cut of the cervical vessels). The liver was dissected, and random samples of all lobes were frozen and stored at -80 °C. Alternatively, liver fragments were fixed in a freshly made fixative solution (4 % w/v, 0.1 M formaldehyde, pH 7.2) for 24 h and followed for light microscopy and immunofluorescence after embedding in Paraplast plus (Sigma-Aldrich, St Louis, MO, USA), and sectioned with a thickness of 5 µm. The sections were stained with hematoxylin-eosin (HE), Sirius red, or immunofluorescence.

Plasmatic measurements. After centrifugation (712 *xg*, 10 min), plasmatic hormone concentrations were measured (enzyme-linked immunosorbent assay kits, ELISA) to assess insulin (EZRMI-13K, Millipore, Merck, Temecula, CA, USA), leptin (EZML-82K), and adiponectin (EZMADP-60K, Millipore, Merck, Temecula, CA, USA) concentrations (TP-Reader ELX800, BioTek Instruments Winooski, VT, USA).

Liver

a) HSCs identification. For antigen retrieval, sections were submitted to citrate buffer (pH 6.0, at 60 °C for 20 min), glycine 2 %, and blocking buffer (PBS/5 % BSA), then incubated overnight at 4 °C with anti-Reelin (1:100, AB78540, Abcam, Eugene, OR, USA), and anti-alpha-actin smooth muscle (SMA) (1:100, AB7817; Abcam). The sections were incubated with fluorochrome-conjugated secondary antibody IgG-Alexa 488 and IgG-Alexa 546 (Invitrogen, Molecular Probes, Carlsbad, CA, USA), diluted 1:50 in PBS/1 % BSA at room temperature for one hour. The slides were mounted (Slow Fade Antifade, Invitrogen) after rinsing in PBS. Digital images were taken with a Nikon Confocal Laser Scanning Microscopy (Model C2; Nikon Instruments, Inc., New York, USA).

b) Steatosis assessment and liver fibrosis. The volume density of fat in the hepatocyte (Vv [fat, hepatocyte] %) was estimated by stereology (point-counting method) in a sample of at least ten fields peranimal obtained from nonconsecutive random sections of the liver (Mandarim-de-Lacerda & Del-Sol, 2017). Therefore, Vv [fat, hepatocyte] was estimated on HE-stained sections as described elsewhere (Catta-Preta *et al*., 2011). Other random sections of the liver were observed after Sirius red staining to study the collagen fiber distribution (Marinho *et al*., 2017).

c)Real-time quantitative polymerase chain reaction (RT qPCR). Total RNA of the liver (30 mg) was extracted (Trizol, Invitrogen, CA, USA), and quantified (spectroscopy, Nanovue, GE Life Sciences), then one microgram was treated with DNAse I. Then, oligo (dT) primers for mRNA and Superscript III reverse-transcriptase were applied to the synthesis of the first-strand cDNA (thermocycler CFX96 (Bio-Rad, Hercules, CA, USA, and SYBR Green mix). The endogenous beta-actin was used to normalize the expression of the selected genes. After the pre-denaturation and polymerase-activation program (4 min at 95 °C), 44 cycles of 95 °C for 10 s and 60 °C for 15 s were followed by a melting curve program (60–95 °C, the heating rate of 0.1 °C/s). The expression intensities of the genes were analyzed by qPCR, and the ratio of relative mRNA expression was calculated using 2-DDCT - DCT as the difference between the number of cycles (CT).

Statistical analysis. The data were shown as the means and standard deviations, and differences between the groups were tested with the unpaired t-test and Welch correction (GraphPad Prism v. 9.1 for Windows, La Jolla, CA, USA).

RESULTS

The three-month-old *ob/ob* mice showed an increased body mass by +110 % compared to the WT mice of the same age, as expected. Therefore, *ob/ob* animals showed higher plasma insulin (+70 %) and lower leptin (-60 %) concentrations than WT animals. Besides, adiponectin (an anti-inflammatory adipokine) was reduced in *ob/ob* mice compared to the WT mice (-50 %) (Table I).

Inflammation and apoptosis in the liver. The liver mRNA relative expressions of inflammation-related genes in the *ob/ob* group were higher than the WT group: Tnf-alpha (+230 %), Il 6 (+130 %). Moreover, the hepatocyte death rate in *ob/ob* mice was higher and linked with Caspase 3 increase than the WT mice (Table I).

Table I. Differences between the wild-type mouse (WT) and leptin-deficient obese (ob/ob) mouse (n = 10/group, Welch t-test).

Data	WT	ob/ob	*P*
Body mass, g	26.46±1.09	55.90±2.27	<0.000
Plasmatic analyses			
Adiponectin, 10^6	22.28±2.50	11.16±1.04	0.000
Insulin, UI/L	14.66±0.17	25.23±0.12	<0.000
Leptin, 10^2 pg/mL	13.23±1.94	5.01±0.82	0.000
Liver qPCR			
Caspase 3, mRNA, a.u.	1.17±0.09	3.41±0.16	<0.000
Il 6, mRNA, a.u.	1.07±0.07	2.49±0.28	<0.000
Tnf-alpha, mRNA, a.u.	1.11±0.09	3.64±0.18	<0.000

Abbreviations: a.u., arbitrary units; Il, interleukin; mRNA, messenger ribonucleic acid; P, probability; Tnf, tumor necrosis factor.

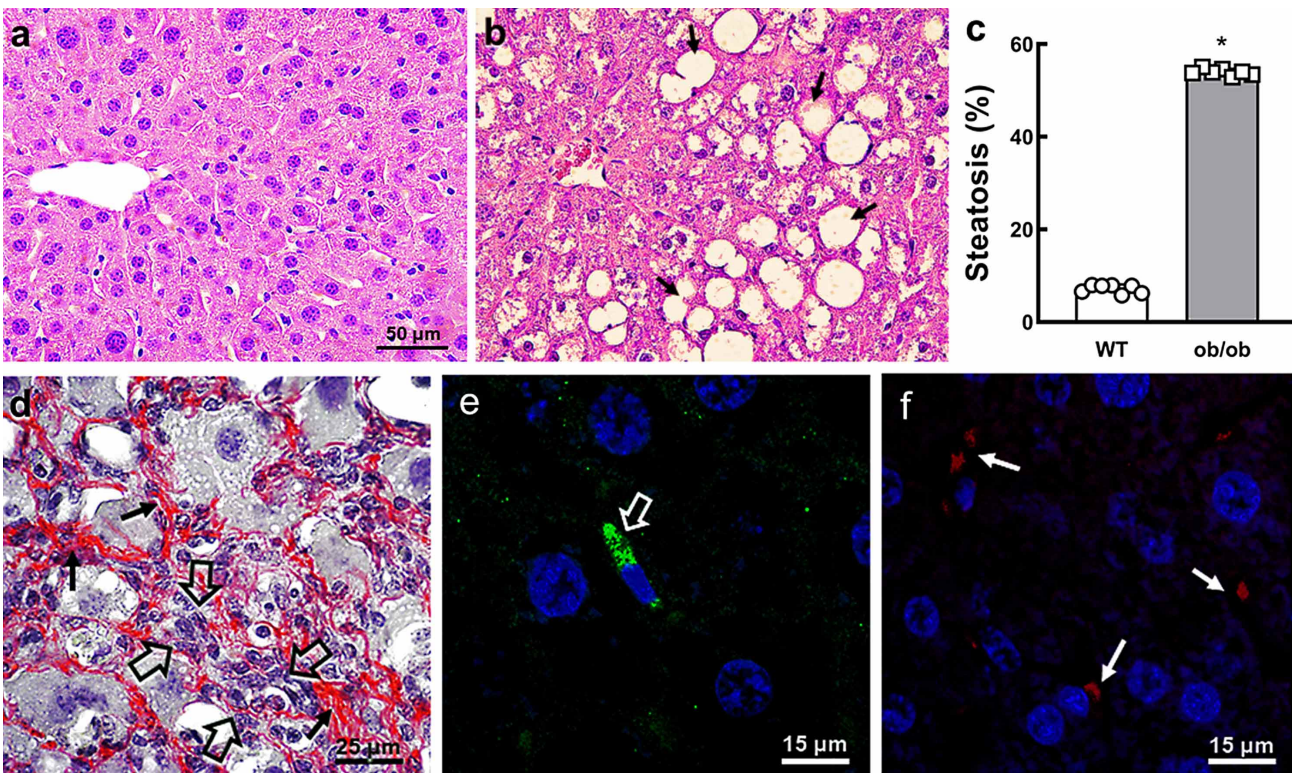

Fig. 1. Photomicrographs of the liver and steatosis assessment, interstitial collagen deposition, and immunofluorescence for activated hepatic stellate cell detection. (a) Wild-type (WT) mouse - liver tissue with an apparent typical structure, without sinusoidal dilatation or significative hepatocyte fat droplet accumulation. (b) Ob/ob mouse - liver tissue shows disarray and macro (arrows) and micro-steatosis with hepatocyte ballooning (a and b, same magnification, H-E stain). (c) The steatosis in the liver was estimated by stereology (mean ± SD, *P<0.001 comparing WT and ob/ob). (d) The ob/ob mouse - large interstitial collagen fibers network was identified by the Sirius red stain (red color, black arrows) and inflammatory infiltrates (open black arrows). (e) Possible activated stellate cell (like myofibroblasts) was identified with an anti-Reelin antibody (green color, open white arrow). (f) Possible activated stellate cells were likewise identified with anti-alpha-SMA antibody (red color, white arrows) (e and f, immunofluorescence, and confocal laser scanning microscopy). (n= 10/group).

Liver steatosis and HSCs activation . Liver steatosis (+650 %) and ballooned hepatocytes were more significant in the *ob/ob* mice than in the WT group (Figs. 1a-c). Besides, the *ob/ob* mice, but not the WT mice, showed a marked accumulation of collagen fibers in the liver stroma, interspersed with focuses of inflammatory infiltrates (Fig. 1d). Accordingly, there was a positive labeling/signal for alpha-SMA and Reelin immunostaining, suggesting HSCs activation in the *ob/ob* mice, but not the WT mice (Figs. 1e-f).

Liver lipogenesis and profibrogenic markers. The genes linked with lipid metabolism and lipogenesis were more expressed in the *ob/ob* group than in the WT one: Ppar-gamma (+275 %, Fig. 2a), Cidec (+50 %, Fig. 2b), Srebp1c (+190 %, Fig. 2c), and Fas (+175 %, Fig. 2d). These data corroborate the pattern of hepatic steatosis developed in the *ob/ob* animals.

The relative mRNA expressions connected to pro-fibrogenesis were higher in the *ob/ob* mice compared to the WT mice: Col1a1 (+780 %, Fig. 2e), Smad3 (+160 %, Fig. 2f), Yap1 (+140 %, Fig. 2g), Pdgfr-beta (+80 %, Fig. 2h), alpha-actin (+610 %, Fig. 2i), and Tgf-beta1 (+275 %, Fig. 2j). These findings are relevant, and the interaction between Smad3, Yap1, Pdgfr-beta, and Tgf-beta1 are original data for understanding liver fibrosis mechanisms in leptin-deficient obese mice.

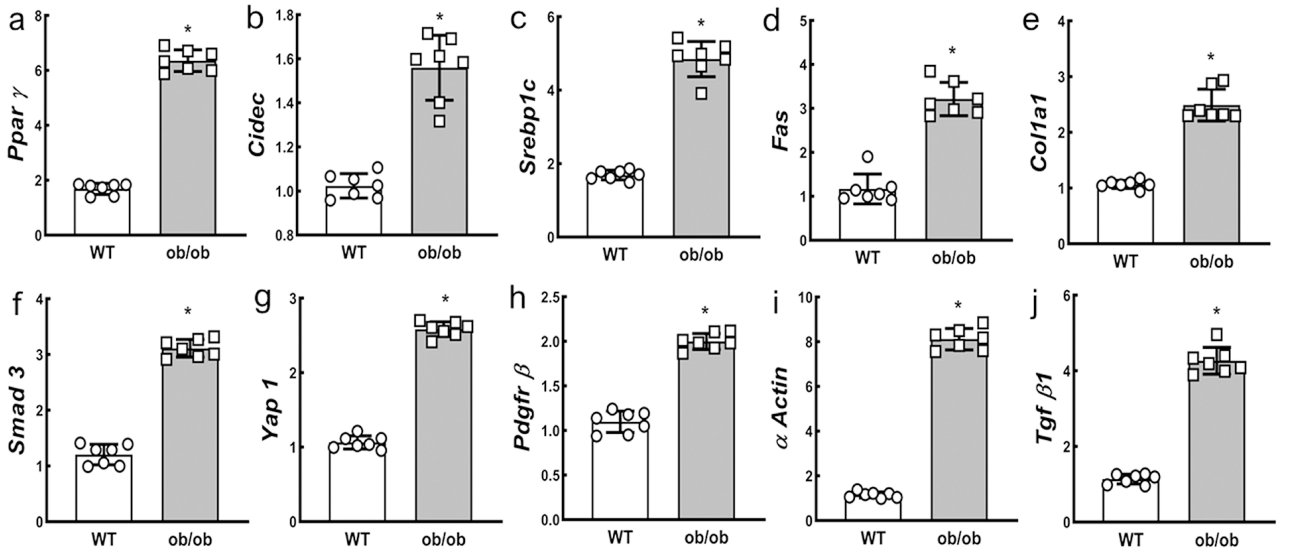

Fig. 2. Gene expressions in the liver (relative mRNA expression in arbitrary units): MARKERS OF LIPOGENESIS. (a) Ppar gamma (peroxisome proliferator-activated receptor-gamma). (b) Cidec (cell death-inducing DFFA-like effector c). (c) Srebp1c (sterol regulatory element-binding protein). (d) Fas (fatty acid synthase). MARKERS OF PRO-FIBROGENESIS. (e) Col1a1 (collagen type I). (f) Smad3 (smad proteins). (g) Yap1 (yes-associated protein). (h) Pdgfr-beta (protein platelet-derived growth factor receptor). (i) Alpha-actin; (j) Tgf-beta1 (transforming growth factor). Means ± SD, *P<0.001 comparing WT and ob/ob. (n= 10/group).

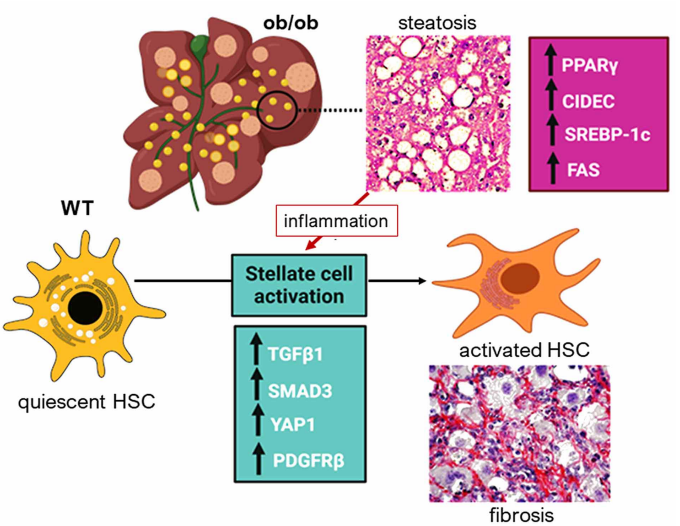

Fig. 3. Graphical abstract. The liver structure is standard in WT mice, presenting no steatosis or fibrosis and quiescent HSCs. Liver steatosis is marked in ob/ob mice, linked to higher expression of Ppar-gamma, Cidec, Srbp-1c, and Fas, and inflammation. Therefore, activated HSCs mediated the pro-fibrogenic factors Tgf-beta1, Smad3, Yap1, and Pdgfr-beta, increasing collagen deposition fibers, generating fibrosis (figure created by FFM using the website https://app.biorender.com).

DISCUSSION

The inflammation and the increased flux of lipids in the liver might generate noteworthy changes in the *ob/ob* mouse hepatocytes. Also, interactions between pro- and anti-inflammatory cytokines such as TNF-alpha, adiponectin, and other cytokines are likely to play critical functions in liver disease development and progression (Mak *et al*., 2019).

Peroxisome proliferator-activated receptors (PPAR) -gamma is a ligand-activated transcription factor involved in the transcriptional regulation of lipid metabolism, glucose homeostasis, energy balance, and inflammation (Choudhary *et al*., 2019). The ell death-inducing DFFA-like effector c (CIDEC) is a direct target gene of Ppar-gamma. It generates high hepatic triacylglycerol levels, primarily by increasing the transcription of genes related to lipogenesis, and the suppression of Ppar-gamma-Cidec affects cell differentiation, maturation and reduces adipogenesis (Martins *et al*., 2020). Ppar-gamma enhanced by miR-942 might decrease the HSCs activation in hepatic fibrosis as an attempt to regulate fibrosis (Tao *et al*., 2020). In the study, both Ppar-gamma and Cidec were higher in the *ob/ob* mice.

Several factors might be enhanced, promoting HSCs survival, proliferation, and fibrosis, including transforming growth factor (TGF) -beta, connective tissue growth factor, ligands for Toll-like receptors 2 and 9, pro-inflammatory cytokines, platelet-derived growth factor (PDGF), and leptin (Choi *et al*., 2010). The PDGF receptor is a chemoattractant that drives HSCs proliferation and migration. Pdgfr-alpha showed a pro-fibrotic role in HSCs during a chronic liver injury in vivo via regulation of HSCs survival and migration, affecting the immune microenvironment, especially macrophages clearing dying hepatocytes (Kikuchi *et al*., 2020). Pdgfr-beta is absent in quiescent HSCs but upregulated in an early stage of liver injury (activating factors such as Tgf-beta1 stimulate the transcriptional induction of Pdgfr-beta in quiescent HSCs (Tsuchida & Friedman, 2017). Here, hepatic Pdgfr-beta was notably higher in *ob/ob* mice.

Sterol regulatory element-binding protein (SREBP)-1c is the dominant insulin-stimulated isoform responsible for inducing lipogenic gene expression and promoting hepatic fatty acid synthase (FAS) (Ferre & Foufelle, 2010). Srebp1c activation impacts the partition of triacylglycerol accumulation in the liver, resulting in adipose tissue remodeling by inflammation, fibrosis, and insulin resistance (Ohno *et al*., 2018). Srebp1c and Fas increased significantly in the *ob/ob* group, corroborating the report of dyslipidemia in *ob/ob* mice (Duong *et al*., 2018).

The expression of pro-fibrotic genes increased significantly in the *ob/ob* liver. Tgf-beta is usually the most potent fibrogenic cytokine released by numerous liver cells in a latent form (Hellerbrand *et al*., 1999). Tgf-beta binding and phosphorylation of the type I receptor induces phosphorylation of downstream SMAD proteins, mainly SMAD3. Activation of Smad3 during HSCs activation makes the transcription of type I and type III collagen (Breitkopf *et al*., 2006), and it was enhanced in the *ob/ob* animals. On the contrary, Il-10 might mitigate hepatic fibrosis by inducing senescence of activated HSCs in vivo, linked to the p53 signaling pathway (Guo *et al*., 2020).

Tribbles homolog 2 (TRIB2) is an oncogene implicated in various cancers, including liver cancer, and colocalizes with alpha-SMA in fibrotic liver tissues (Xiang *et al*., 2021). Yes-associated protein (YAP, a mediator of the Hippo pathway) type 1 contributes to benign steatosis progression to fibrosis through interaction with Tgf-beta1 and Smad3. YAP/transcriptional co-activators with the PDZ-binding motif are mechano-regulators of Tgf-beta-Smad signaling that increase hepatic fibrosis (Mannaerts *et al*., 2015). TRIB2 promoted YAP stabilization, nuclear localization, and subsequent fibrotic gene expression. TRIB2 interacted with YAP to recruit phosphatase 1A and YAP dephosphorylation (Xiang *et al*., 2021). These genes were highly expressed in the liver of the *ob/ob* group.

Alpha-SMA labeling, a marker for a subset of activated fibrogenic cells, allows the detection of activated HSCs (Carpino *et al*., 2005). Reelin labeling was also used to underline HSCs' identification (Kobold *et al*., 2002). In the study, liver sections in *ob/ob* mice were labeled by both anti-alpha-SMA and anti-Reelin in the fibrotic zones, but not in the WT mice. Moreover, the alpha-actin gene expression was higher in the *ob/ob* group's liver than the WT group.

In conclusion, the study demonstrated original findings that contribute to a better understanding of the mechanisms related to liver changes in leptin-deficient obese animals. In the *ob/ob* animals, there were increased gene expressions involved with lipogenesis (Ppar-gamma, Cidec, Srebp1c, and Fas), pro-fibrogenesis (Tgf-beta1, Smad3, Yap1, Pdgfr-beta), pro-inflammation (Tnf-alpha, and Il 6), and apoptosis (Caspase 3). The results in obese *ob/ob* animals provide a clue to the events in humans. In a translational view, controlling these targets can help mitigate the hepatic effects of human obesity and NAFLD progression to NASH.

Author contributions

FFM, CAML – conceptualization. FFM - roles/writing - original draft. FFM, VSM, JJC, MDS, MBA, CAML - data

curation, investigation, methodology, formal analysis. MBA, CAML - funding acquisition; project administration; resources. CAML - supervision; validation; writing - review & editing.

Funding. The study was supported by Conselho Nacional de Desenvolvimento Científico e Tecnológico (Brazil) (CNPq, Grant No 302.920/2016-1 to CAML, and 305.865/2017-0 and 401001/2016-4 to MBA), Fundação Carlos Chagas Filho de Amparo à Pesquisa do Estado do Rio de Janeiro (Faperj, Grant No E-26/202.935/2017 to CAML, and E-26/202.795/2017 to MBA). These foundations had no interference in the accomplishment and submission of the study.

Conflict of interest statement. The authors declare that there are no conflicts of interest.

ACKNOWLEDGMENTS

We thank the skillful laboratory staff (laboratory of morphometry, metabolism, and cardiovascular disease, www.lmmc.uerj.br) at the University of the State of Rio de Janeiro for always prompt to help in the analyses.

MARTINS, F. F.; SOUZA-MELLO, V.; CARVALHO, J. J.; DEL SOL, M.; AGUILA, B. M. & MANDARIM-DE-LACERDA, C. A. Lesión estructural del hígado en ratones con deficiencia de leptina (*ob/ob*): Lipogénesis, fibrogénesis, inflamación y apoptosis . *Int. J. Morphol., 39(3)*:732-738, 2021.

RESUMEN: La enfermedad del hígado graso no alcohólico (HGNA) puede progresar de la esteatosis a esteatohepatitis no alcohólica (ENA), alcanzando un estado de cirrosis y posiblemente carcinoma hepatocelular. Se estudió el hígado de ratones C57BL / 6J de tres meses de edad (tipo salvaje, grupo WT, n = 10) y ratones obesos con deficiencia de leptina (grupo *ob/ob*, n = 10), centrándose en los mecanismos asociados con la activación de las células estrelladas hepáticas (HSC) y profibrogénesis. El hígado de los animales obesos *ob/ob* mostró esteatosis, aumento de la expresión génica de la lipogénesis, inflamación, aumento de la expresión génica proinflamatoria, infiltrado inflamatorio y posible apoptosis ligada a una alta expresión de Caspasa 3. En ratones *ob/ob*, las secciones de hígado se marcaron en las zonas fibróticas con anti-alfa-actina de músculo liso (alfa-SMA) y anti-Reelin, pero no en los ratones WT. Además, la expresión del gen alfa-SMA fue mayor en el hígado del grupo *ob/ob* que en el grupo WT. Las expresiones génicas profibrogénicas fueron paralelas a la inmunofluorescencia anti-alfa-SMA y anti-Reelin, lo que sugiere la activación de las HSC. En los animales *ob/ob*, hubo un aumento de las expresiones génicas involucradas con la lipogénesis (receptor activado por proliferador de peroxisoma gamma, efector c similar a DFFA inductor de muerte celular, proteína de unión al elemento regulador de esterol-1c y sintasa de ácidos grasos), pro-fibrogénesis (factor de crecimiento transformante beta 1, proteínas Smad-3, proteína-1 asociada a Yes, receptor beta del factor de crecimiento derivado de plaquetas de proteínas), proinflamación (factor de necrosis tumoral alfa e interleucina-6) y apoptosis (caspasa 3).). En conclusión, los resultados en animales obesos *ob/ob* proporcionan una pista de los eventos en humanos. Desde un punto de vista traslacional, el control de estos objetivos puede ayudar a mitigar los efectos hepáticos de la obesidad humana y la progresión de HGNA a ENA.

PALABRAS CLAVE: Esteatosis; Célula estrellada; Fibrosis; Microscopía confocal; Estereología.

REFERENCES

Aguila, M. B.; Ornellas, F. & Mandarim-de-Lacerda, C. A. Nutritional research and fetalprogramming: parental nutrition influences the structure and function of the organs. *Int. J. Morphol., 39*: 327-34, 2021.

Bettermann, K.; Hohensee, T. & Haybaeck, J. Steatosis and steatohepatitis: complex disorders. *Int. J. Mol. Sci., 15*:9924-44, 2014.

Breitkopf, K.; Godoy, P.; Ciuclan, L.; Singer, M. V. & Dooley, S. TGF-beta/Smad signaling in the injured liver. *Z. Gastroenterol., 44*:57-66, 2006.

Carpino, G.; Morini, S.; Ginanni Corradini, S.; Franchitto, A.; Merli, M.; Siciliano, M.; Gentili, F.; Onetti Muda, A.; Berloco, P.; Rossi, M.; Attili, A. F. & Gaudio, E. Alpha-SMA expression in hepatic stellate cells and quantitative analysis of hepatic fibrosis in cirrhosis and in recurrent chronic hepatitis after liver transplantation. *Dig. Liver Dis., 37*:349-56, 2005.

Catta-Preta, M.; Mendonca, L.S.; Fraulob-Aquino, J.; Aguila, M.B. & Mandarim-de-Lacerda, C.A. A critical analysis of three quantitative methods of assessment of hepatic steatosis in liver biopsies. *Virchows Arch., 459*:477-85, 2011.

Cho, E. H. Succinate as a Regulator of Hepatic Stellate Cells in Liver Fibrosis. *Front. Endocrinol. (Lausanne), 9*:455, 2018.

Choi, S.S.; Syn, W.K.; Karaca, G.F.; Omenetti, A.; Moylan, C.A.; Witek, R.P.; Agboola, K.M.; Jung, Y.; Michelotti, G.A. & Diehl, A.M. Leptin promotes the myofibroblastic phenotype in hepatic stellate cells by activating the hedgehog pathway. *J. Biol. Chem., 285*: 36551-60, 2010.

Choudhary, N. S.; Kumar, N. & Duseja, A. Peroxisome Proliferator-Activated Receptors and Their Agonists in Nonalcoholic Fatty Liver Disease. *J. Clin. Exp. Hepatol., 9*:731-9, 2019.

Duong, M.; Uno, K.; Nankivell, V.; Bursill, C. & Nicholls, S.J. Induction of obesity impairs reverse cholesterol transport in *ob/ob* mice. *PLoS One, 13*:e0202102, 2018.

Ferre, P. & Foufelle, F. Hepatic steatosis: a role for de novo lipogenesis and the transcription factor SREBP-1c. *Diabetes Obes. Metab., 12 Suppl 2*:83-92, 2010.

Fuchs, S.; Yusta, B.; Baggio, L.L.; Varin, E.M.; Matthews, D. & Drucker, D.J. Loss of Glp2r signaling activates hepatic stellate cells and exacerbates diet-induced steatohepatitis in mice. *J. C. I. Insight, 5*, 2020.

Guo, Q.; Chen, M.; Chen, Q.; Xiao, G.; Chen, Z.; Wang, X. & Huang, Y. Silencing p53inhibits interleukin 10-induced activated hepatic stellate cell senescence and fibrotic degradation *in vivo*. *Exp. Biol. Med.* (Maywood), (doi: 10.1177/1535370220960391): 1535370220960391, 2020.

Gupta, G.; Khadem, F. & Uzonna, J. E. Role of hepatic stellate cell (HSC)-derived cytokines in hepatic inflammation and immunity. *Cytokine, 124*:154542, 2019.

Hellerbrand, C.; Stefanovic, B.; Giordano, F.; Burchardt, E. R. & Brenner, D.A. The role of TGFbeta1 in initiating hepatic stellate cell activation *in vivo*. *J. Hepatol., 30*:77-87, 1999.

Khomich, O.; Ivanov, A.V. & Bartosch, B. Metabolic Hallmarks of Hepatic Stellate Cells in Liver Fibrosis. *Cells*, 9, 2019.

Kikuchi, A.; Singh, S.; Poddar, M.; Nakao, T.; Schmidt, H. M.; Gayden, J. D.; Sato, T.; Arteel, G. E. & Monga, S.P . Hepatic Stellate Cell-Specific Platelet-Derived Growth Factor Receptor-alpha Loss Reduces Fibrosis and Promotes Repair after Hepatocellular Injury. *Am. J. Pathol., 190*:2080-94, 2020.

Kobold, D.; Grundmann, A.; Piscaglia, F.; Eisenbach, C.; Neubauer, K.; Steffgen, J.; Ramadori, G. & Knittel, T. Expression of reelin in hepatic stellate cells and during hepatic tissue repair: a novel marker for the differentiation of HSC from other liver myofibroblasts. *J. Hepatol., 36*:607-13, 2002.

Lua, I.; Li, Y.; Zagory, J. A.; Wang, K. S.; French, S. W.; Sevigny, J. & Asahina, K. Characterization of hepatic stellate cells, portal fibroblasts, and mesothelial cells in normal and fibrotic livers. *J. Hepatol., 64*:1137-46, 2016.

Mak, L. Y.; Lee, C. H.; Cheung, K. S.; Wong, D. K.; Liu, F.; Hui, R. W.; Fung, J.; Xu, A.; Lam, K. S.; Yuen, M. F. & Seto, W. K. Association of adipokines with hepatic steatosis and fibrosis in chronic hepatitis B patients on long-term nucleoside analogue. *Liver Int., 39*:1217-25, 2019.

Mandarim-de-Lacerda, C.A. & del-Sol, M. Tips for Studies with Quantitative Morphology (Morphometry and Stereology). *Int. J. Morphol., 35*:1482-94, 2017.

Mannaerts, I.; Leite, S. B.; Verhulst, S.; Claerhout, S.; Eysackers, N.; Thoen, L. F.; Hoorens, A.; Reynaert, H.; Halder, G. & van Grunsven, L. A. The Hippo pathway effector YAP controls mouse hepatic stellate cell activation. *J. Hepatol., 63*:679-88, 2015.

Marinho, T. S.; Kawasaki, A.; Bryntesson, M.; Souza-Mello, V.; Barbosa-da-Silva, S.; Aguila, M. B. & Mandarim-de-Lacerda, C. A. Rosuvastatin limits the activation of hepatic stellate cells in diet-induced obese mice. *Hepatol. Res., 47*:928-40, 2017.

Martin, N.; Ziegler, D.V.; Parent, R. & Bernard, D. Hepatic Stellate Cell Senescence in Liver Tumorigenesis. *Hepatology*, (doi: 10.1002/hep.31556), 2020.

Martins, F. F.; Aguila, M. B. & Mandarim-de-Lacerda, C. A. Eicosapentaenoic and docosapentaenoic acids lessen the expression of PPARgamma/Cidec affecting adipogenesis in cultured 3T3-L1 adipocytes. *Acta Histochem., 122*:151504, 2020.

Ohno, H.; Matsuzaka, T.; Tang, N.; Sharma, R.; Motomura, K.; Shimura, T.; Satoh, A.; Han, S.I.; Takeuchi, Y.; Aita, Y.; Iwasaki, H.; Yatoh, S.; Suzuki, H.; Sekiya, M.;Nakagawa, Y.; Sone, H.; Yahagi, N.; Yamada, N.; Higami, Y. & Shimano, H. Transgenic Mice Overexpressing SREBP-1a in Male *ob/ob* Mice Exhibit Lipodystrophy and Exacerbate Insulin Resistance. *Endocrinology, 159*:2308-23, 2018.

Sferra, R.; Vetuschi, A.; Pompili, S.; Gaudio, E.; Speca, S. & Latella, G. Expression of pro-fibrotic and anti-fibrotic molecules in dimethylnitrosamine-induced hepatic fibrosis. *Pathol. Res. Pract., 213*:58-65, 2017.

Tao, L.; Wu, L.; Zhang, W.; Ma, W. T.; Yang, G. Y.; Zhang, J.; Xue, D.Y.; Chen, B. & Liu, C. Peroxisome proliferator-activated receptor gamma inhibits hepatic stellate cell activation regulated by miR-942 in chronic hepatitis B liver fibrosis. *Life Sci., 253*:117572, 2020.

Tsuchida, T. & Friedman, S. L. Mechanisms of hepatic stellate cell activation. *Nat. Rev. Gastroenterol. Hepatol., 14*:397-411, 2017.

Xiang, D.; Zhu, X.; Zhang, Y.; Zou, J.; Li, J.; Kong, L. & Zhang, H. Tribbles homolog 2 promotes hepatic fibrosis and hepatocarcinogenesis through phosphatase 1A-Mediated stabilization of yes-associated protein. *Liver Int*., (doi: 10.1111/liv.14782), 2021.

Zhang, X.; Zhang, X.; Huang, W. & Ge, X. The role of heat shock proteins in the regulation of fibrotic diseases. *Biomed. Pharmacother., 135*:111067, 2020.

Corresponding author:
Prof. Dr. Carlos Alberto Mandarim-de-Lacerda
Laboratório de Morfometria, Metabolismo e
Doença Cardiovascular
Centro Biomédico
Instituto de Biologia
Universidade do Estado do Rio de Janeiro
Av 28 de Setembro 87 fds, 20551-030
Rio de Janeiro,
RJ - BRAZIL

E-mail: mandarim@uerj.br
mandarim.ca@gmail.com

Website: www.lmmc.uerj.br.

Received: 05-02-2021
Accepted: 25-04-2021

Fabiane Ferreira Martins:
Email: fabibhex@gmail.com Orcid: 0000-0002-3831-6604)

Vanessa Souza-Mello
Email: v.souzamello@gmail.com Orcid: 0000-0002-2510-9569

Jorge Jose de Carvalho
Email: jjcarv@gmail.com Orcid: 0000-0002-9426-6381

Mariano del Sol
Email: mariano.delsol@ufrontera.cl Orcid: 0000-0003-3686-6757

Marcia Barbosa Aguila
Email: mbaguila@uerj.br Orcid: 0000-0003-3994-4589

Carlos Alberto Mandarim-de-Lacerda
Email: mandarim@uerj.br Orcid: 0000-0003-4134-7978